AN NMR STUDY OF EREMOMYCIN AND ITS DERIVATIVES

FULL ^{1}H AND ^{13}C ASSIGNMENT, MOTIONAL BEHAVIOR, DIMERIZATION AND COMPLEXATION WITH AC-D-ALA-D-ALA

GYULA BATTA* and FERENC SZTARICSKAI*

Research Group for Antibiotics of the Hungarian Academy of Sciences,
P.O. Box 70, H-4042 Debrecen, Hungary

KATALIN E. KÖVÉR

BIOGAL Pharmaceutical Works,
H-4010 Debrecen, Hungary

CHRISTIAN RÜDEL

Ruhr-Universität Bochum Fakultät für Chemie, Lehrstul für Analytische Chemie,
Postfach 102148, D-4630, Bochum 1, Germany

TATJANA F. BERDNIKOVA

Institute of New Antibiotics, Academy of Medical Science,
Bolshaya Pirogovskaya 11, Moscow 119 867, USSR

(Received for publication May 7, 1991)

Complete ^{1}H and ^{13}C NMR assignments are presented for eremomycin (**1**) and some of its desglycosylated derivatives **2**, **3** and compared to the structurally closely related glycopeptide vancomycin. Primary structure and stereochemistry of eremomycin is corroborated by the present high field total correlation spectroscopy, NOESY and heteronuclear multiple-bond correlation NMR methods. A rough motional characterization of the title compound is attempted by ^{13}C-T_1 and ^{13}C-$\{^{1}H\}$ NOE measurements. Dimerization of eremomycin is observed both in DMSO-d_6 - CCl_4 and D_2O solutions. Complexation with cell wall analogue dipeptide Ac-D-Ala-D-Ala is also demonstrated.

Eremomycin[1~3] or A82846A[4,5] belongs to the rich family of the vancomycin-ristocetin group of glycopeptide type of antibiotics and are closely related to orienticins[6~8]. Its activity is 2~10 times higher in the antibacterial spectrum than those of ristocetin and vancomycin, while the toxicity of this novel compound is several times lower than that of vancomycin[9,10]. Eremomycin is presently under clinical trial.

The structure of eremomycin has been verified in several independent works[3~5,11], however no detailed NMR analysis appeared till now.

In the present work we analyze the ^{1}H and ^{13}C NMR spectra of eremomycin hydrochloride (**1**) (Fig. 1), deseremosaminyleremomycin (**2**: "f"-eremosaminyl unit is removed from **1**), the pseudo-aglycone (**3**: R_2-disaccharide is removed) and the aglycone (**4**). In addition, we studied the motional behavior of eremomycin in D_2O solution by measuring its ^{13}C-T_1 relaxation times and ^{13}C-$\{^{1}H\}$ broadband NOE values (NOEBB). Complexation with Ac-D-Ala-D-Ala was also studied.

Fig. 1. Structure of eremomycin and its desglycosyl derivatives.

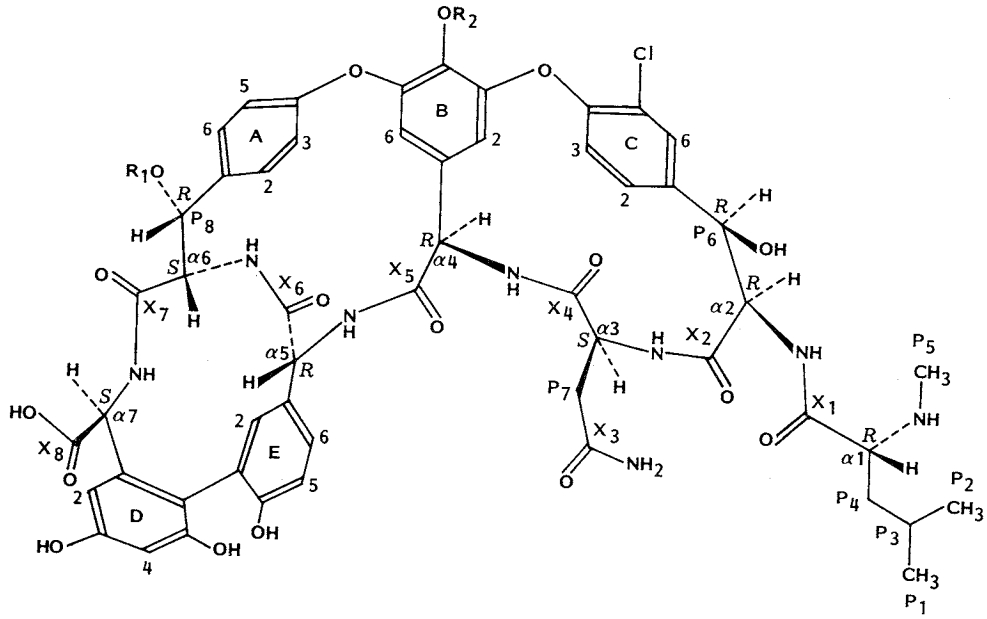

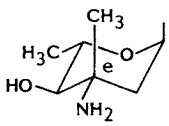

L-Eremosaminyl-
(L-4-*epi*-vancosaminyl)

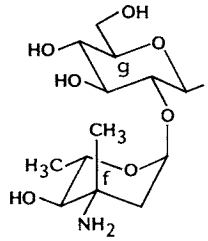

2-*O*-(α-L-Eremosaminyl)-
β-D-glucopyranosyl

Eremomycin (**1**)	R_1 = L-Eremosaminyl	R_2 = 2-*O*-(α-L-Eremosaminyl)-β-D-glucopyranosyl
Deseremosaminyleremomycin (**2**)	R_1 = L-Eremosaminyl	R_2 = β-D-Glucopyranosyl
Pseudo-aglycone (**3**)	R_1 = L-Eremosaminyl	R_2 = H
Aglycone (**4**)	$R_1 = R_2$ = H	

Results and Discussion

In order to obtain reliable ^1H and ^{13}C spectral assignments we carried out the basic 2D chemical shift correlation experiments (COSY and HETCOR) at low field and equipped them with total correlation spectroscopy (TOCSY)[12,13], NOESY and heteronuclear multiple-bond correlation (HMBC)[14] techniques at high field. The analysis of the 2D spectra, and comparison of the 2D chemical shift coordinates of eremomycin and its derivatives with those of vancomycin and its aglycone afforded nearly complete ^1H and ^{13}C assignments for the new compounds.

Aglycoeremomycin (**4**)

Table 1 shows the ^1H and ^{13}C NMR assignments of **4** and aglycovancomycin (AGV)[15,16] in DMSO solution. Most of the carbonyl and aromatic quaternary carbons are assigned by chemical shift comparison. Remaining signals were assigned using standard COSY and HETCOR methods. Assignments of CH signals

Table 1. Comparison of chemical shifts of the aglycones of eremomycin and vancomycin.

No.	Assignment	Aglycoeremomycin (**4**)		AGV (**5**)[15,16]		No.	Assignment	Aglycoeremomycin (**4**)		AGV (**5**)[15,16]	
		δ_C	δ_H	δ_C	δ_H			δ_C	δ_H	δ_C	δ_H
1	x-1	172.01	—	172.6	—	28	C-3	124.16	7.22	124.50	7.26
2	x-8	171.66	—	171.6	—	29	A-2	121.54	6.90	126.80	7.48
3	x-3	170.44	—	170.0	—	30	E-3	121.43	—	121.70	—
4	x-2	169.71	—	169.3	—	31	A-3	120.50	7.06	123.10	7.23
5	(x-5)[a]	169.10	—	168.1	—	32	D-6	117.90	—	118.0	—
6	(x-6)[a]	168.75	—	167.5	—	33	E-5	116.10	6.70	116.40	6.76
7	x-7	167.60	—	167.0	—	34	A-5	112.56	6.85	126.10	—
8	x-4	166.27	—	166.0	—	35	B-2	106.52	5.60	109.40	5.65
9	D-3	156.91	—	157.1	—	36	B-6	106.02	5.35	106.50	5.20
10	D-5	156.20	—	156.4	—	37	D-2	105.92	6.27	106.20	6.30
11	E-4	154.73	—	154.9	—	38	D-4	102.41	6.39	102.80	6.45
12	A-4	154.14	—	149.6	—	39	(P-6)[c]	71.61	5.16	71.50	5.14
13	C-4	150.23	—	150.2	—	40	(P-8)[c]	71.29	5.13	71.50	5.14
14	B-5	149.16	—	148.5	—	41	α-6	61.98	4.18	62.00	4.22
15	B-3	147.83	—	147.9	—	42	α-1	60.70	3.60	59.80	3.99
16	A-1	139.48	—	141.9	—	43	α-2	58.89	4.77	59.50	4.92
17	C-1	139.48	—	139.3	—	44	α-7	56.50	4.48	56.80	4.49
18	D-1	135.97	—	136.1	—	45	α-5	54.51	5.65	53.90	5.72
19	E-2	135.62	7.15	135.8	7.16	46	α-4	53.40	4.52	55.00	4.47
20	B-1	134.20	—	134.2	—	47	α-3	50.99	4.25	51.30	4.31
21	B-4	128.89	—	128.90	—	48	P-4	39.72	1.60	39.70	1.75
22	C-6	128.02	7.48	128.50	7.49	49	P-7	35.97	2.11/	38.60	2.18/
23	(A-6)[b]	126.80	7.55	127.50	7.86				2.65		2.50
24	(C-2)[b]	126.56	7.60	128.20	7.60	50	P-5	32.23	2.49	31.20	2.65
25	E-1	126.14	—	127.50	—	51	P-3	23.77	1.73	23.90	1.75
26	C-5	126.00	—	126.20	—	52	(P-1)[d]	22.26	0.92	22.90	0.94
27	E-6	125.23	6.78	125.50	6.81	53	(P-2)[d]	22.26	0.88	22.40	0.90

Other ^1H signals in **4** (ppm): ~9.4 (2H, s, OH/Ph), 8.67 (1H, d, 2-NH), 8.58 (1H, d, 4-NH), 8.51 (1H, d, 7-NH), 8.06 (1H, d, 5-NH), 6.55 (1H, d, 6-NH), 5.47 (1H, d, 3-NH), 5.90 (2H, br s, 2×OH), 35 mg of **4** was dissolved in 500 μl DMSO-d_6 and measured 70°C. ^{13}C chemical shifts are referenced to the solvent signal (δ_C 39.5 ppm) while ^1H shifts are referenced to internal TMS.

Exchangeable assignments are labeled with identical indices attached to parenthesis.

in ring "A" are exchangeable because of strong couplings at 200 MHz in the *para*-substituted benzene ring. More importantly, most assignments of the α-CH signals, and P-6/P-8 fit perfectly to AGV proton and carbon chemical shift coordinates. Only two minor exceptions were found; α-1 and α-4 showed 0.9 and −1.6 ppm (^{13}C) and 0.39 ppm (^1H) deviations from the reference AGV. This fact suggests that stereochemistry may be identical at all of the nine asymmetric centers in **4** and AGV, as it is usual in this group of antibiotics (*e.g.* for orienticins[5,6]). However, this suggestion should be strictly confirmed by NOE distance constraints.

Eremomycin and Its Derivatives

The ^1H (Fig. 2) and ^{13}C NMR data of eremomycin (D_2O, 70°C) are summarized in Table 2. Non-protonated carbon atoms were identified by 1D quantitative, exclusive detection of quaternaries, using a modified spin echo sequence with long recycle delay, and 2D long-range heteronuclear correlations[14] without chemical shift comparison.

Protons and the attached carbon atoms could be unambiguously assigned by combined COSY (not shown), TOCSY (Fig. 3A, B, C), NOESY (Fig. 4), heteronuclear correlation methods HETCOR (Fig. 5)

Fig. 2. 500 MHz ^{1}H NMR survey spectrum of eremomycin in D_2O solution at 70°C and a partial 200 MHz ^{1}H NMR spectrum of eremomycin at 80°C showing the small splittings (*ca.* 1 Hz) due to $^4J_{f2ax,Me\text{-}f3}$ coupling.

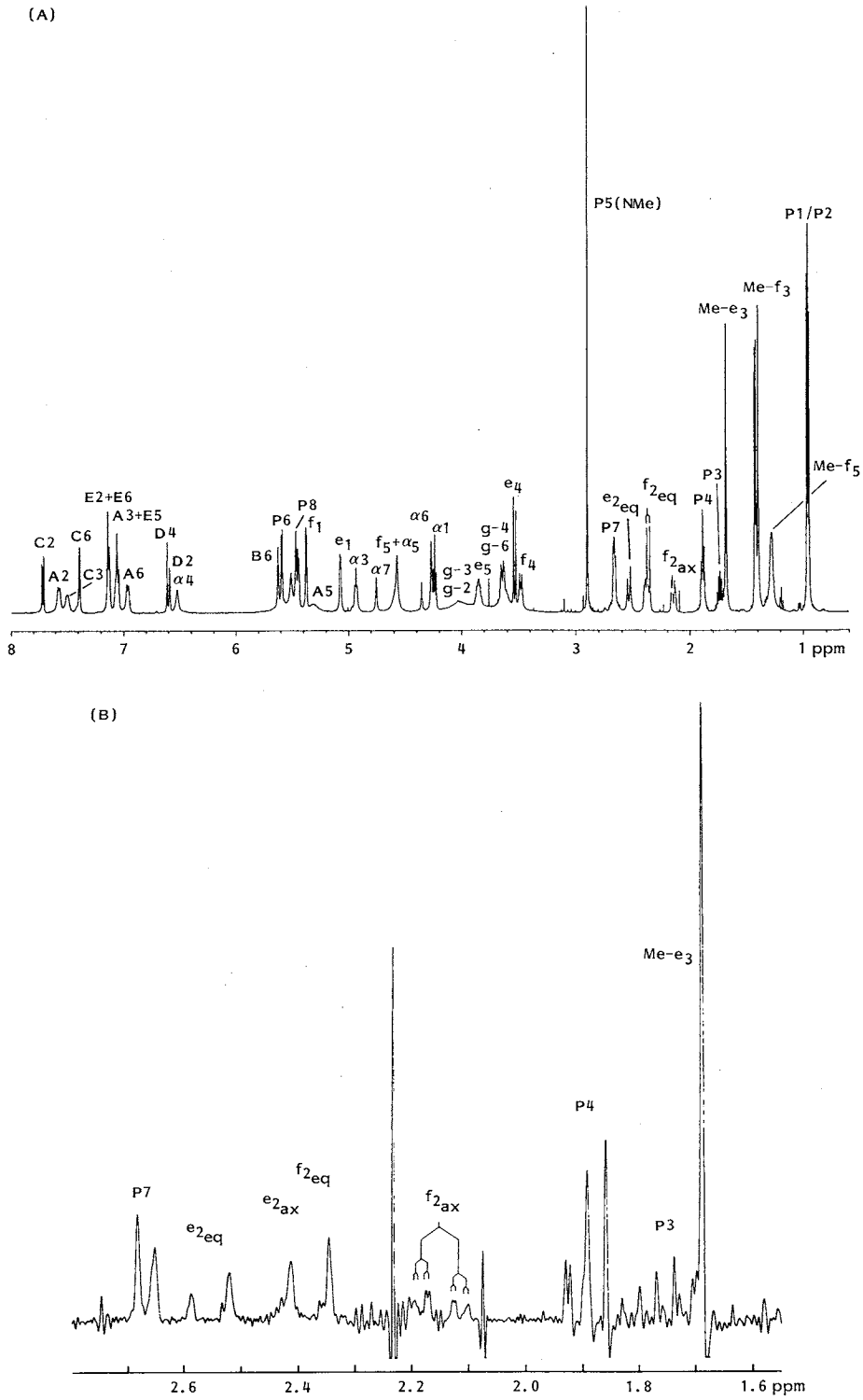

Table 2. ^{1}H and ^{13}C assignments of eremomycin as verified by through-bond and through-space connectivities.

No.	δ_C	δ_H	Assignment	$^{n}J_{CH}$ couplings to protons (70°C, 500 MHz)	Short range homonuclear NOE (25°C, 400 MHz) connectivities to protons	^{13}C (70°C, 50.3 MHz) T_1 (seconds)	NOEBB (±20%)
1	176.40	—	x-8	α-8		2.13	48
2	174.46	—	x-3	α-3, P-7		2.10	78
3	172.11	—	x-5	α-4		1.41	48
4	171.80	—	x-6	α-5, α-6		—	34
5	171.29	—	x-4	α-3, P-7		(1.78)	(63)
6	171.23	—	x-1	α-1, α-2, P-4		(1.78)	(63)
7	169.39	—	x-2	α-2, α-3		1.90	43
8	167.88	—	x-7	α-6, α-7		—	54
9	157.21	—	D-3	D-2, D-4		(2.28)	(19)
10	157.21	—	(B-3)[a]			(2.28)	(19)
11	156.41	—	(A-4)[a]			2.73	46
12	155.68	—	D-5	D-4		2.12	29
13	155.06	—	E-4	E-2, E-5, E-6		3.54	41
14	153.34	—	B-5	B-6		3.45	57
15	150.76	—	C-4	C-2, C-6		1.98	47
16	138.20	—	C-1	C-3, α-2, P-6		(1.68)	(62)
17	137.92	—	D-1	α-7		(1.68)	(62)
18	136.31	7.16	E-2	E-6, α-5		0.158	101
19	134.92	—	(B-1)[b]	B-6		1.18	59
20	134.22	—	(B-4)[b,c]			—	54
21	133.83	—	(A-1)[c]			1.69	63
22	130.70	7.39	C-6	C-2, P-6	e-2_{ax}, e-2_{eq}, P-6	0.43	105
23	129.42	7.57	A-2	A-6, P-8	α-6, P-8, A-3	0.137	103
24	128.79	6.96	A-6	P-8	e-1, e-2_{eq}	0.116	89
25	128.35	—	C-5	C-2, C-3, C-6		1.12	62
26	127.60	7.13	E-6	E-2, α-5	α-6, α-7	0.113	100
27	127.28	7.71	C-2	C-6, P-6	P-5	0.136	104
28	126.56	—	E-1	E-5, α-5		1.25	65
29	125.56	7.49	C-3			0.158	95
30	123.55	7.06	A-3		A-2	0.119	77
31	122.17	—	E-3	E-5		—	101
32	122.09	5.32 br	A-5			0.198	65
33	119.01	7.04	E-5			0.150	114
34	118.27	—	D-6	D-2, D-4, E-2		—	31
35	109.09	6.59	D-2	D-4, α-7		0.151	82
36	107.71	5.51	(B-2)[d]			0.079	81
37	104.80	5.63	(B-6)[d]			0.108	120
38	103.87	6.61	D-4	D-2		0.168	68
39	102.30	5.55 br	g-1			0.162	112
40	98.03	5.37	f-1	f-2_{eq}, f-2_{ax}	f-2_{eq}, f-2_{ax}	0.137	110
41	93.27	5.08	e-1	e-2_{eq}, P-8	e-2_{eq}, e-2_{ax}, A-6	0.143	117
42	80.00	~4.03 br	g-2	f-1		0.203	142
43	77.14	~4.03 br	(g-3)[e]		f-1	0.206	105
44	76.44	~3.79 br	(g-5)[e]			0.155	110
45	75.62	3.53	e-4	e-1, Me-e_3, Me-e_5	e-2_{ax}, Me-e_3, Me-e_5	0.120	117
46	75.30	5.47	P-8		α-6, A-2	0.148	108
47	75.20	3.48	f-4	f-2_{eq}, Me-f_5	f-2_{ax}, Me-f_5	0.155	97
48	71.78	5.59	P-6	C-2, C-6, α-2	C-6	0.162	96
49	70.33	~3.63 br	g-4			0.111	106
50	67.03	3.85	e-5	e-1, e-4	Me-e_3, Me-e_5, P-8	0.192	113
51	66.62	4.58	f-5	f-1		0.140	104
52	62.31	4.27	α-6		α-7, P-8, A-2, E-6	0.107	105
53	61.76	4.24	α-1	P-3, P-2, P-4, P-5	P-1, P-2, P-4, P-5	(0.168)	(126)
54	61.76	3.64	g-6			(0.168)	(126)

Table 2. (Continued)

No.	δ_C	δ_H	Assignment	$^nJ_{CH}$ couplings to protons (70°C, 500 MHz)	Short range homonuclear NOE (25°C, 400 MHz) connectivities to protons	^{13}C (70°C, 50.3 MHz) T_1 (seconds)	NOEBB (±20%)
55	59.83	5.45	α-2			0.196	102
56	59.46	4.75	α-7	D-2	α-6, E-2	0.178	111
57	57.45	—	e-3	e-1, e-2_{eq}, e-4, Me-e_3		1.93	91
58	57.11	—	f-3	f-1, f-2_{eq}, Me-f_3		2.64	90
59	55.34	4.56	α-5	E-2, E-6		0.139	115
60	55.21	6.53	α-4	B-6		0.203	92
61	53.10	4.94	α-3	P-7	e-2_{eq}, Me-e_3, P-7	0.141	117
62	39.76	1.88	P-4	α-1, P-1, P-2, P-3	α-1, P-1, P-2	0.115	108
63	39.40	2.14 2.36	f-2_{ax} f-2_{eq}		f-1, f-4 f-1, Me-f_3	0.173	151
64	39.08	2.39 2.54	e-2_{ax} e-2_{eq}		e-1, e-4, C-6 e-1, Me-e_3, A-6, α-3, C-6	0.103	109
65	36.95	2.67	P-7		α-3		
66	32.66	2.89	P-5	α-1	α-1, C-2, P-1, P-2	1.26	126
67	24.53	1.73	P-3	α-1, P-1, P-2, P-4	P-1, P-2	0.63	132
68	22.78	0.96	(P-1)[f]	P-4	α-1, P-3, P-4, P-5	1.31	167
69	22.03	0.95	(P-2)[f]	P-4	α-1, P-3, P-4, P-5	1.31	171
70	18.85	1.68	Me-e_3	e-2_{eq}	e-2_{eq}, e-5, α-3	0.508	134
71	18.51	1.40	Me-f_3	f-2_{eq}, f-2_{ax}	f-2_{eq}	0.469	118
72	17.91	1.42	Me-e_5	e-4	e-4, e-5	0.522	130
73	17.59	1.28	Me-f_5		f-4	0.516	96

One bond ^1H-^{13}C connectivities were measured with the conventional HETCOR method at 50.3/200.13 MHz.

Long-range ^1H-^{13}C connectivities were determined in two different multiple bond heteronuclear correlation (MBHC) experiments using 70 or 40 mseconds delay periods for generation of heteronuclear multiple quantum coherence at 500/125 MHz.

Through-space NOESY connectivities were measured at 400 MHz using a mixing time of 170 mseconds. Phase sensitive spectra were processed with a novel baseline correction routine[29].

Spin lattice relaxation times T_1 and broadband heteronuclear NOE's (NOEBB) were evaluated at 50.3 MHz.

All measurements were carried out in D_2O solution at 70°C, except the NOESY, where t=25°C was more useful to avoid the zero cross NOE region. External TMS was used as reference signal for ^{13}C NMR, while proton shifts are referenced to internal DSS.

Ambiguities concerning assignments or measured values are indicated with brackets.

and HMBC (Fig. 6). A comparison of 2D HETCOR coordinates of eremomycin (**1**) (Table 2) with its derivatives (**2**~**4**) (Tables 1 and 3), supported the proposed assignments.

The following structural features are worth to be noted on the basis of NMR data.

Carbohydrate Moieties

In both eremosaminyl units ("e" and "f") the anomeric protons are equatorial *i.e.* their anomeric configurations are α. This is substantiated by the $^1J_{C1,H1}$ values of 170.5 and 172.5 Hz. This fact is also supported by a 2D NOE measurement at 25°C (Fig. 4). Cross peaks of similar intensity between the anomeric proton and both the axial and equatorial (2-H_{ax}, 2-H_{eq}) protons were found. The same NOE map indicated 2,4-diaxial arrangement between f-4 and f-2_{ax} (e-4 and e-2_{ax}). Identical assignments were also found in eremosamine[17,18] for the 2-ax and 2-eq protons. In the "g" D-glucopyranosyl unit we found $^1J_{C1,H1}$=165 Hz, indicating a typical β-anomeric configuration. Corroborating this finding in the derivative **2** we found $^3J_{g1,g2}\approx$9 Hz in a double quantum (DQ)-filtered COSY experiment showing a *trans*-diaxial vicinal proton-proton coupling. The e-3 and f-3 configurations are safely assigned by a 3,5-diaxial NOE

Fig. 3. Partial 500 MHz TOCSY spectra of eremomycin (D_2O, 70°C).

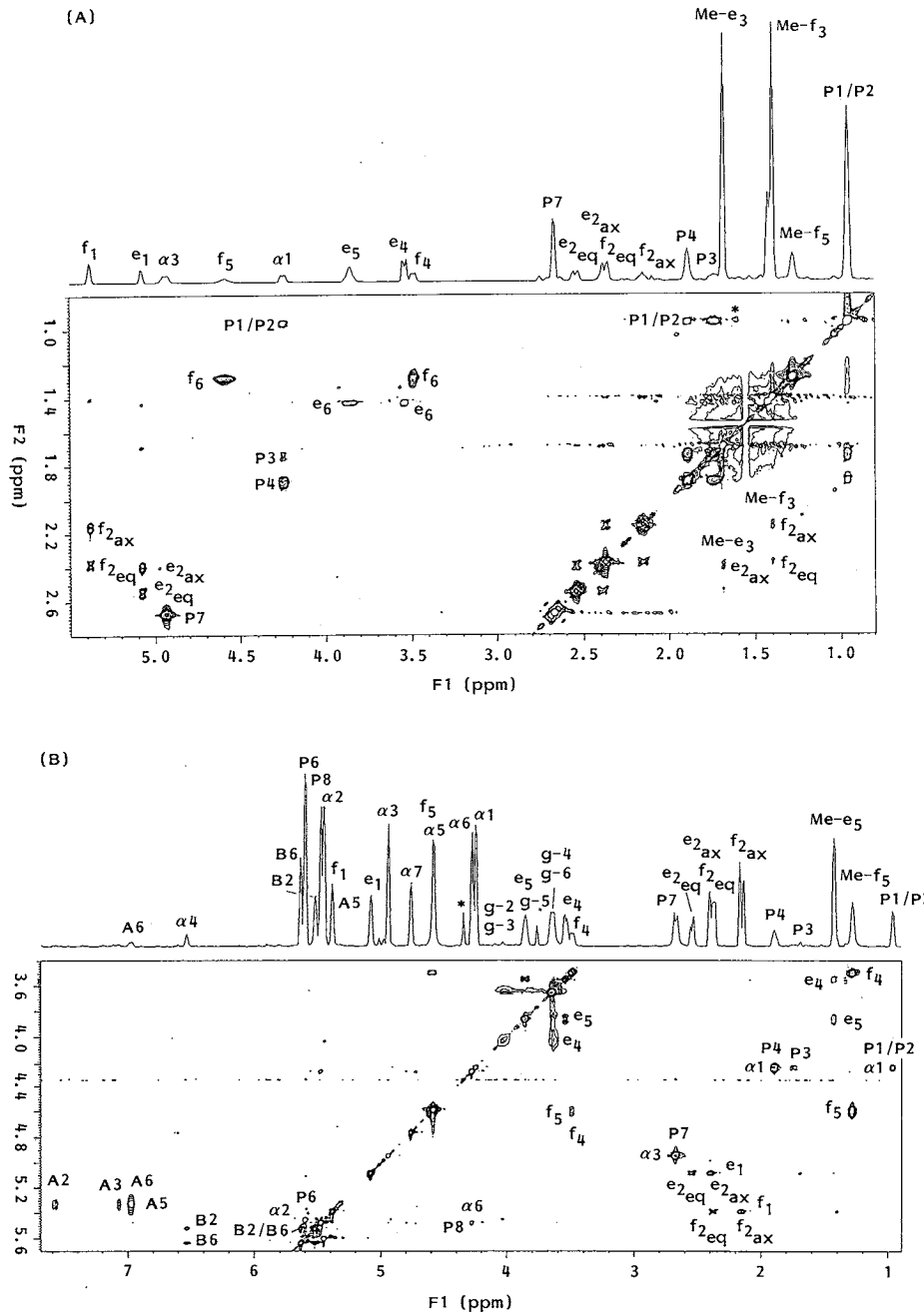

between the 3-methyl groups and the e-5 and f-5 protons.

The e-4 (f-4) configurations of the eremosaminyl units are reversed, as compared to the vancosaminyl unit of vancomycin, according to a $^3J_{H4,H5} \approx 9$ Hz vicinal coupling. The same conclusion can be obtained by a *ca.* 5 ppm ^{13}C downfield shift at f-2 in eremomycin, as compared to vancomycin, due to a γ-gauche effect.

An interesting four-bond long-range coupling of *ca.* 1 Hz has been observed between the Me-f3 group

Fig. 3. (Continued)

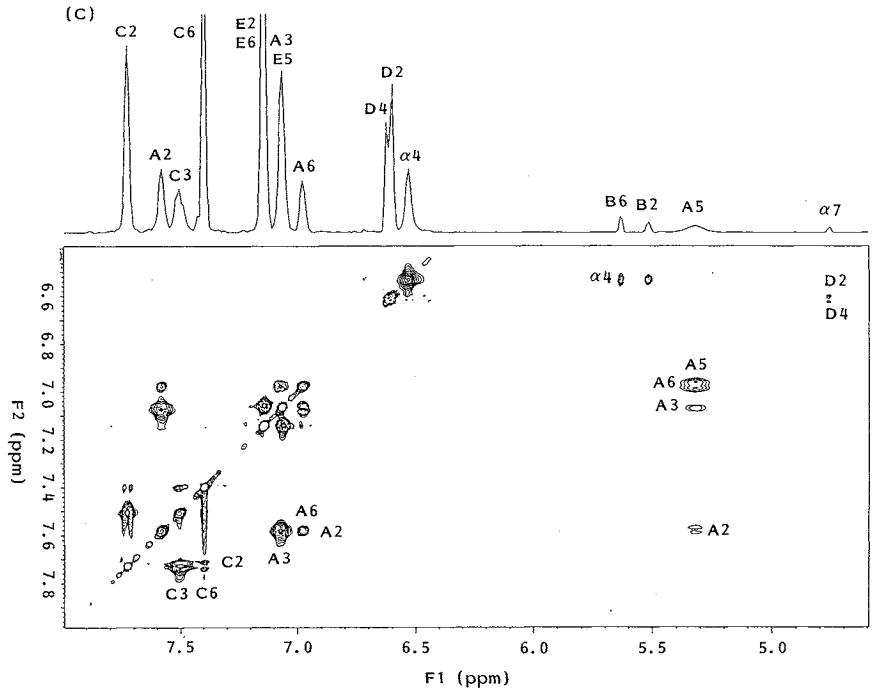

Residual HDO signal was presaturated during the 2 seconds relaxation delay, which was preceded by a homospoil-90-homospoil sequence. A trim pulse of 2 mseconds was followed by a 80 mseconds MLEV-17 spin lock field. Acquisition time of 0.233 second in 2 K data table provided 4,400 Hz spectral window. Experiments were incremented 512 times. Hypercomplex data were processed in the phase sensitive manner.

Note connectivities between A-5 and A-2, A-3, A-6 protons, α-4 and B-2, B-6 protons, α-7 and D-2, D-4 protons (Fig. 3C), Me-f_3 and f-2_{ax} protons, Me-e_3 and e-2_{ax} protons (Fig. 3A). Some of these four bond connections were also found in magnitude mode COSY experiments but not in the phase sensitive double quantum filtered COSY spectra, because of the antiphase nature of small splittings.

and f-2_{ax} protons, as shown in the 1D partial 200 MHz spectrum (Fig. 2) and also in the TOCSY spectrum (Fig. 3A). The $^3J_{g\text{-}2,f\text{-}1}$ interglycosidic carbon-proton coupling detected in the HMBC experiment verified the bond type[19] of the disaccharide unit.

Comparing the ^{13}C and ^1H chemical shifts of eremomycin and deseremosaminyleremomycin (**2**) we found that upon removal of the "f" ring all values remained practically unchanged except the "g" glucopyranosyl unit. This observation suggests a similar average conformation for the core atoms of **1** and **2**.

Aglycone of Eremomycin

The eight carbonyls in the ^{13}C spectrum were safely assigned based on detection of $^2J_{Xn,an-1}$ and $^3J_{Xn,an}$ long range carbon-proton couplings (Fig. 6 and Table 2). Ambiguity between x-3 and x-2 was resolved by the NOEBB heteronuclear NOE. The highest value among the carbonyls (x-3) can be attributed to higher mobility of asparagine and/or more efficient dipolar relaxation through the CH_2 (P-7) group.

Long-range heteronuclear couplings of aromatic carbons were essential for verifying their assignments and for tracing out the carbon skeleton of this antibiotic. Such important connectivities are *e.g.* A-2, A-6→P-8; C-1→α-2, P-6; D-1→α-7; E-1, E-2→α-5; D-6→E-2.

Protonated carbons were assigned by HETCOR (Fig. 5) following the full proton assignment. However,

Fig. 4. Phase sensitive (TPPI) NOESY experiment of eremomycin at 400 MHz in D_2O (25°C) solution.

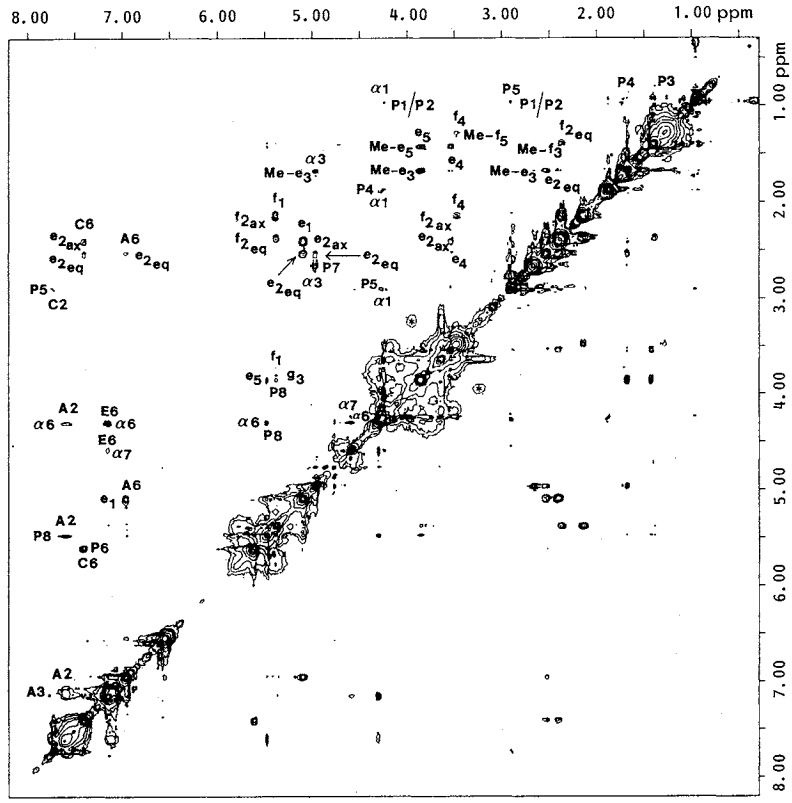

Acquisition time was 0.135 second using 1 K data table. 24 transients were accumulated for each of the 256 incremented experiments. A mixing time of 0.17 second was randomized to *ca.* ±5%. Note interunit connectivities due to formation of stable dimers, *e.g.* C-6→e-2_{ax}, e-2_{eq} and α-3→e-2_{eq}, Me-e_3.

When partially deuterated eremomycin (30 minutes after dissolution in D_2O) was measured by NOESY or ROESY experiment (spinlock time = 150 mseconds) we found dipolar couplings of the 5-NH signal to α-4 and D-4 protons.

it was still useful to refer to long-range carbon-proton connectivities of α-CH and side chain carbons; *e.g.* α-1→P-4; α-3→P-7; α-4→B-6; α-5→E-2; α-7→D-2; P-6→α-2, C-2, C-6; P-4, P-5→α-1.

Of course, some carbon assignments remained exchangeable due to signal overlap or similar coupling network.

Motional Behavior of Eremomycin

A rough motional characterization of **1** has been attempted by ^{13}C-T_1 relaxation time measurements and broadband (BB) ^{13}C-{^1H} NOE measurement at 50 MHz (appropriate data are also shown in Table 2). As the heteronuclear NOE values are far from their theoretical maximum of *ca.* 200%, we found, that average correlation times in D_2O solution at 70°C are well outside the extreme narrowing regime. The lack of homonuclear NOE's at 200 MHz also suggested that molecular motions are around the zero-cross ^1H-{^1H} NOE region.

Supposing the simplest spectral density function[20] in the form of

Fig. 5. ^{1}H-^{13}C one bond chemical shift correlation of eremomycin (D_2O, 70°C) at 200.13/50.3 MHz using BIRD type ^{1}H-^{1}H decoupling in F1 dimension.

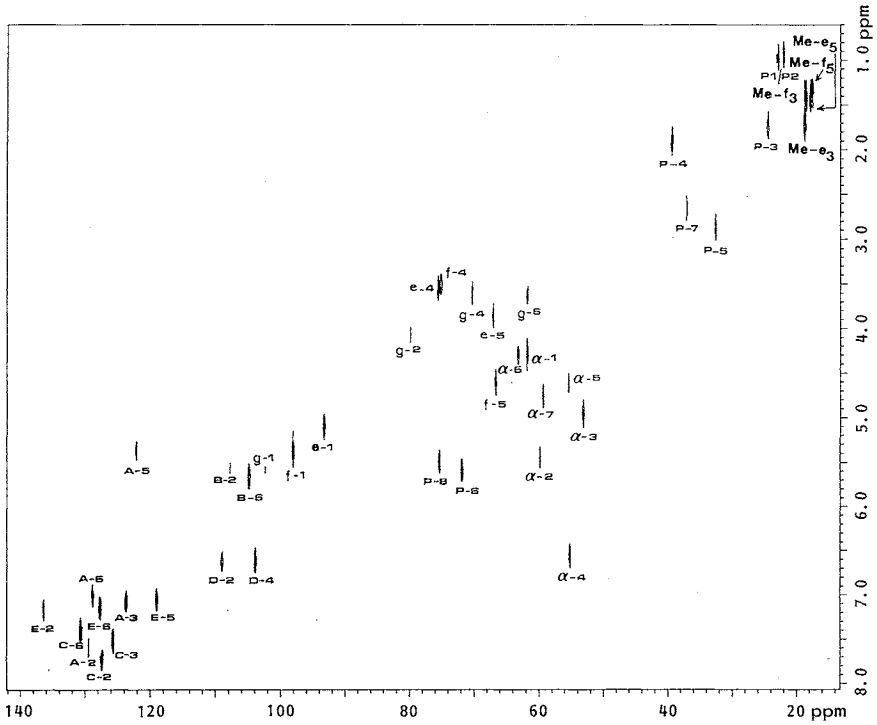

The $1/2J_{CH}$ period was set to 3.2 mseconds, while a 2.0-msecond refocussing delay allowed detection of all multiplicities. 1 K data tables were used for acquisition. 512 transients were accumulated for each of the 64 incremented experiments. A Gaussian weighting function was applied in F2 dimension, while a $\pi/3$ shifted and squared sine bell in the F1 dimension. A power spectrum composed of 256×2 K data points is shown to enhance the signal to noise ratio. However, some broad signals of the D-glucopyranosyl unit (g) are below the plotted level. The missing e-2 and f-2 signals of nonequivalent CH_2 groups were detected in a separate HMQC experiment.

$$J_{(\omega)} = \frac{\langle A(o)^2 \rangle \tau_c}{1 + \omega^2 {\tau_c}^2}$$

and an isotropic reorientation (which are probably oversimplifications), average correlation times were determined for protonated carbons according to the measured nT_1 and NOEBB values. As it is usual, the two methods give different τ_c results, however, they could be roughly estimated. From the relaxation time data we obtain a range of 10^{-11} second $< \tau_c < 10^{-10}$ second while the NOEBB data suggest 4×10^{-10} second $< \tau_c < 10^{-9}$ second.

Flexibility of methyl groups P_1, P_2 and P_5 of the *N*-methylleucine at the *N* terminus are clearly demonstrated, while the aromatic rings in the molecular interior may be restricted in internal motions. WALTHO *et al.* arrived to similar conclusions by studying the antibiotic vancomycin using ^{1}H NMR methods.[21].

These dynamical features of hydrophobic groups may play an important role in the molecular recognition processes of glycopeptide antibiotics[22~27].

Dimerization of Eremomycin and Its Complexation with Ac-D-Ala-D-Ala

Vancomycin and the Ac-D-Ala-D-Ala complex is a classical example of glycopeptide antibiotic and cell

Fig. 6. Heteronuclear multiple bond correlations (HMBC) in eremomycin (D_2O, 70°C) measured at 499.84/125.68 MHz.

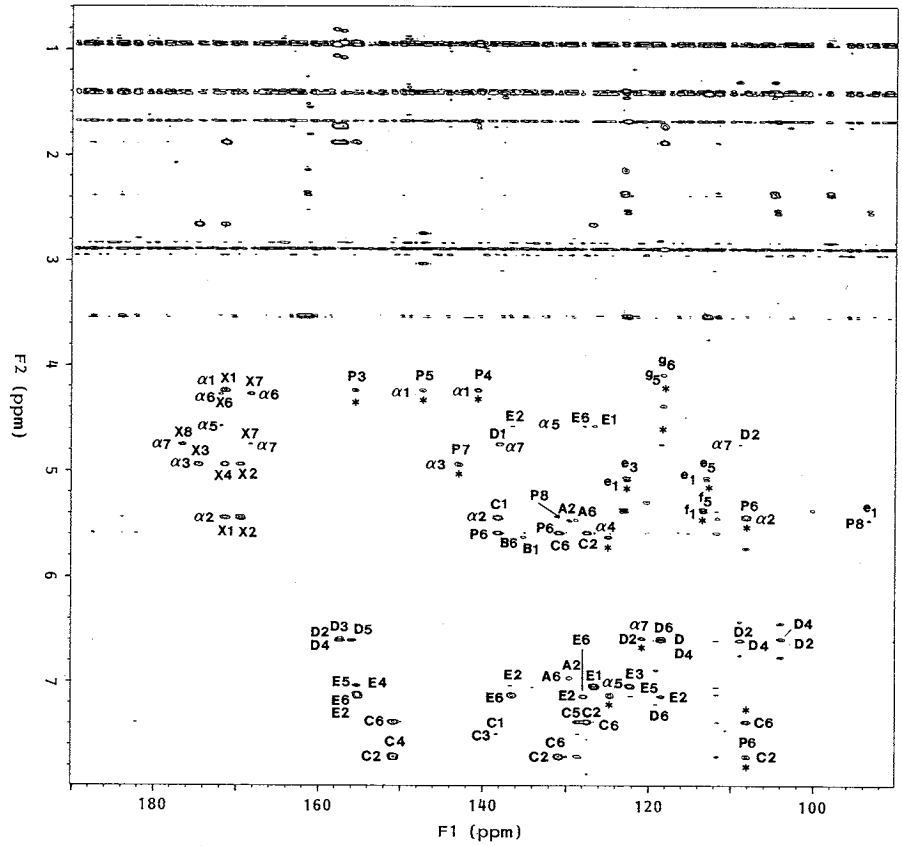

128 transients were accumulated for each of the 512 incremented experiments. Residual HDO signal was saturated during the 3 seconds relaxation delay. A delay of 40 mseconds for preparation of long-range coupling generated multiple quantum coherences was allowed. Signals, which are folded in restricted (100 ppm) ^{13}C spectral window are labeled with asterisks. Folding could be assigned based on a separate experiment with 70 mseconds multiple bond delay and full spectral window.

wall analogue oligopeptide interaction. The most apparent feature of this complexation in the ^1H NMR spectrum is the appearance of the NH-2 signal at *ca.* δ_H 12 ppm due to a strong intermolecular hydrogen bond with the carboxylate anion of the dipeptide.

To the contrary, in pure eremomycin (10 mM concentration, DMSO-CCl_4 (10:3) solution, at 5°C) there is an exchangeable proton signal at 12.8 ppm. It is difficult to deuterate, has a temperature dependence of *ca.*

$$-7.5\frac{\text{ppb}}{^\circ\text{C}},$$

furthermore it broadenes significantly by raising the temperature up to 50°C.

In D_2O solution the lowest-field deuterable signal appears at 9.85 ppm. Deuteration takes some days for this proton, which may be assigned as NH-5 involved in a strong intermolecular H-bond. These findings can be explained by the formation of one or more dimers of eremomycin in D_2O solution as it has been suggested[27] for this groups of antibiotics.

Table 3. ^{13}C NMR chemical shifts (δ_C ppm) of the eremomycin derivatives and vancomycin.

No.	Assignment	2 (D_2O)	3 (D_2O + Acetone-d_6)	Vancomycin[16] (D_2O)	No.	Assignment	2 (D_2O)	3 (D_2O + Acetone-d_6)	Vancomycin[16] (D_2O)
1	x-8	176.0	175.32	177.3	38	D-4	103.84	103.79	103.9
2	x-3	174.35	173.93	175.1	39	g-1	104.71	—	102.3
3	x-5	172.00	171.76	171.2	40	f-1	—	—	98.5
4	x-6	171.80	171.38	169.8	41	e-1	93.25	93.44	—
5	x-1	171.26	171.03	168.0	42	g-2	74.21	—	80.1
6	x-4	171.26	170.78	169.0	43	(g-3)[e]	76.63	—	76.9
7	x-2	169.37	169.20	171.9	44	(g-5)[e]	76.50	—	77.5
8	x-7	168.02	168.01	170.2	45	e-4	75.34	75.53	—
9	D-3	157.20	157.57	157.3	46	P-8	75.34	75.53	72.4
10	(B-3)[a]	156.64	156.56	152.2	47	f-4	—	—	71.8
11	(A-4)[a]	156.06	156.27	149.8	48	P-6	71.65	71.90	72.9
12	D-5	155.80	155.36	155.8	49	g-4	70.02	—	70.3
13	E-4	155.00	151.32	155.0	50	e-5	66.94	66.86	—
14	B-5	153.49	151.32	153.6	51	f-5	—	—	64.9
15	C-4	150.75	148.84	151.4	52	α-6	63.03	62.95	64.1
16	C-1	138.18	138.60	139.5	53	α-1	61.80	61.49	61.7
17	D-1	137.73	137.79	138.5	54	g-6	61.80	—	61.6
18	E-2	136.20	136.48	136.5	55	α-2	59.61	60.10	59.6
19	(B-1)[b]	135.20	134.88	135.9	56	α-7	59.01	58.83	60.4
20	(B-4)[b,c]	134.20	134.39	133.4	57	e-3	57.19	57.32	—
21	(A-1)[c]	133.91	134.39	141.2	58	f-3	—	—	55.6
22	C-6	130.65	130.12	129.6	59	α-5	55.13	55.31	54.9
23	A-2	129.46	129.50	129.1	60	α-4	55.13	55.16	56.0
24	A-6	128.91	129.69	128.7	61	α-3	52.93	52.93	52.5
25	C-5	128.21	128.23	127.5	62	P-4	39.6	39.36	39.6
26	E-6	127.58	127.52	127.3	63	e-2	39.3	39.06	—
27	C-2	127.38	127.52	128.1	64	f-2	—	—	34.0
28	E-1	126.36	126.86	128.1	65	P-7	36.79	37.17	36.5
29	C-3	125.51	125.81	125.3	66	P-5	32.48	32.48	32.9
30	A-3	123.32	123.29	124.7	67	P-3	24.36	24.61	24.9
31	E-3	121.90	122.20	122.2	68	(P-1)[f]	22.66	22.72	23.1
32	A-5	121.80	122.46	127.1	69	(P-2)[f]	21.89	22.25	22.8
33	E-5	118.89	118.57	118.9	70	Me-e_3	18.67	18.63	—
34	D-6	118.20	118.33	118.5	71	Me-f_3	—	—	22.9
35	D-2	108.73	108.47	109.1	72	Me-e_5	17.74	17.99	—
36	(B-2)[d]	107.14	106.53	109.0	73	Me-f_5	—	—	17.1
37	(B-6)[d]	104.71	105.21	106.2					

In D_2O solutions external TMS was used as reference signal for ^{13}C NMR, while proton shifts are referenced to internal DSS.

At one magnitude of order lower concentrations (*i.e.* 0.5~1 mM) we observed these low field NH signals neither in DMSO nor in D_2O solutions, which can be rationalized by a much lower dimer concentration.

As both proton and carbon measurements were carried out in 10~50 mM concentration range, the homo-aggregation is supposed to be total for all NMR measurements.

Evaluation of NOESY data (Fig. 4 and Table 2) led to the same conclusion. Existence of dimer structures is clearly evidenced by strong (short range) intermolecular NOE between C-6 and e-2 methylene group of eremosaminyl unit, and α-3 and e-2_{eq} and Me-e_3 protons.

Further indication of dimer formation is evident from the ^1H NMR spectrum (Fig. 2) showing the broad signals of α-4 and the strikingly high field A-5 protons[27].

For studying the complexation of eremomycin and Ac-D-Ala-D-Ala, 7.78 mg eremomycin was dissolved in 500 μl $(CD_3)_2SO$-CCl_4 (10:3) mixture (~10 mM). 2.02 mg (~20 mM) dipeptide was co-added, and the ^1H NMR spectrum was recorded in the 0~5°C temperature range. The NH-5 signal at 12.8 ppm significantly broadened, while the NH signal at 9.75 ppm was shifted downfield to 11.7 ppm as a very broad singlet. These changes show the presence of new intermolecular hydrogen bridges due to the bound dipeptide, although association may be weaker than for vancomycin[28]. More details on the structure of hetero aggregates will be presented elsewhere.

Experimental

The low field NMR measurements (COSY in magnitude representation, and HETCOR) were obtained with a Bruker WP-200 SY spectrometer operated at 200.13 MHz for protons and 50.3 MHz for carbons. For all ^{13}C measurements shown in Table 2 *ca.* 80~100 mg of substance was dissolved in 1.5 ml solvent and measured in a 10-mm NMR tube. The same solution was used for ^1H NMR measurements using a 5-mm probe. Measuring temperature was 70°C if not otherwise noticed (as for **3**, t=60°C). NOESY experiments were executed with a Bruker AM-400 instrument at 25°C. Double quantum filter (DQF)-COSY, TOCSY, heteronuclear multiple-quantum correlation (HMQC) and HMBC spectra were obtained using a Varian UNITY-500 spectrometer (499.84 MHz for protons and 125.68 MHz for carbons).

Specific details of 2D experiments can be found in the figure captions. ^{13}C-T_1 values of Table 2, were obtained at 50.3 MHz by the usual inversion recovery method under broadband proton decoupling. 10 seconds recycle delay was allowed between consecutive sequences. The variable delay list contained 9 elements in increasing steps. NOEBB values were obtained in difference experiments (with and without broadband ^1H decoupling). Also 10 seconds was used for ^{13}C-{^1H} NOE build up. For data evaluation the interferograms were multiplied by a strong exponential function (5 Hz line broadening) and the peak amplitudes were used instead of integral values.

Acknowledgments

Financial support by the Hungarian Academy of Sciences (Grants OTKA 298 and 1144) are gratefully acknowledged.

We thank Drs. E. HOFFMANN and P. SÁNDOR (Varian Associates, Darmstadt) for their kind help with the TOCSY, HMQC and HMBC spectra.

References

1) GAUSE, G. F.; M. G. BRAZHNIKOVA, A. V. LAIKO, M. A. SVESHNIKOVA, T. P. PREOBRAZHENSKAYA, G. B. FEDOROVA, V. N. BORISOVA, I. V. TOLSTYKH, M. S. YURINA, L. S. POKRAS, L. E. GOLDBERG, I. V. MALKOVA & E. S. STEPANOVA: Eremomycin, a novel polycyclic glycopeptide antibiotic. Antibiot. Med. Biotechnol. 32: 571~576, 1987
2) BERDNIKOVA, T. F.; N. L. TOKAREVA, E. A. ABRAMOVA, N. Y. DOKSHINA, N. P. POTAPOVA & N. N. LOMAKINA: Structure of aglycone of eremomycin, a novel antibiotic belonging to the group of polycyclic glycopeptides. Antibiot. Chemother. (Moscow) 33: 566~570, 1988
3) GAUSE, G. F.; M. G. BRAZHNIKOVA, N. N. LOMAKINA, T. F. BERDNIKOVA, G. B. FEDOROVA, N. L. TOKAREVA, V. N. BORISOVA & G. BATTA: Eremomycin—new glycopeptide antibiotic: Chemical properties and structure. J. Antibiotics 42: 1790~1799, 1989
4) HUNT, A. H.; J. L. OCCOLOWITZ, M. DEBONO & R. M. MOLLOY: A82846, a new glycopeptide complex, produced by Amycolatopsis orientalis. 3. Structure determination. Program and Abstracts of the 28th Intersci. Conf. on Antimicrob. Agents Chemother. No. 976, p. 282, Los Angeles, Oct. 23~26, 1988
5) NAGARAJAN, R.; D. M. BERRY, A. H. HUNT, J. L. OCCOLOWITZ & A. A. SCHABEL: Conversion of antibiotic A82846B to Orienticin A and structural relationships of related antibiotics. J. Org. Chem. 54: 983~986, 1989
6) TSUJI, N.; M. KOBAYASHI, T. KAMIGAUCHI, Y. YOSHIMURA & Y. TERUI: New glycopeptide antibiotics. I. The structures of orienticins. J. Antibiotics 41: 819~822, 1988
7) TSUJI, N.; T. KAMIGAUCHI, M. KOBAYASHI & Y. TERUI: New glycopeptide antibiotics: II. The isolation and structures of chloroorienticins. J. Antibiotics 41: 1506~1510, 1988
8) NAGARAJAN, R.; D. M. BERRY & A. A. SCHABEL: The structural relationships of A82846B and its hydrolysis

products with chloroorienticins A, B and C. J. Antibiotics 42: 1438~1440, 1989
9) GOLDBERG, L.; E. S. STEPANOVA, T. P. VERTOGRADOVA, L. A. SHEVNYUK & N. G. SHEPELEVTSEVA: Preclinical toxicological studies of novel antibiotic eremomycin I. Acute toxicity in laboratory animals. Antibiot. Med. Biotechnol. 32: 910~915, 1987
10) MALKOVA, I. V.: Experimental studies of antibacterial activity and chemotherapeutic efficiency of eremomycin, a novel glycopeptide antibiotic. Antibiot. Chemother. (Moscow) 34: 52~56, 1989
11) BATTA, G.; K. E. KÖVÉR, T. F. BERDNIKOVA & F. SZTARICSKAI: Eremomycin—a novel glycopeptide antibiotic. The use of dipolar interactions. European Experimental NMR Conference, 9th: Abstracts. p. 77, Bad Aussee, Austria, May 16~20, 1988
12) BRAUNSCHWEILER, L. & R. R. ERNST: Coherence transfer by isotropic mixing: Application to proton correlation spectroscopy. J. Magn. Reson. 53: 521~528, 1983
13) DAVIS, D. G. & A. BAX: Assignment of complex ^{1}H NMR spectra via two-dimensional homonuclear Hartmann-Hahn spectroscopy. J. Am. Chem. Soc. 107: 2820~2821, 1985
14) MÜLLER, L.: Sensitivity enhanced detection of weak nuclei using heteronuclear multiple quantum coherence. J. Am. Chem. Soc. 101: 4481~4484, 1979
15) WILLIAMS, D. H. & J. R. KALMAN: Structural and mode of action studies on the antibiotic vancomycin. Evidence from 270-MHz proton magnetic resonance. J. Am. Chem. Soc. 99: 2768~2774, 1977
16) BONGINI, A.; J. FEENEY, M. P. WILLIAMSON & D. H. WILLIAMS: Assignment of the carbon-13 spectrum of vancomycin and its derivatives. J. Chem. Soc. Perkin Trans. II 1981: 201~206, 1981
17) LOMAKINA, N. N.; N. L. TOKAREVA & N. P. POTAPOVA: Structure of eremosamine, an amino sugar from eremomycin. Antibiotiki 33: 726~729, 1988
18) HUNT, A. H.; R. M. MOLLOY, M. DEBONO & J. L. OCCOLOWITZ: Isolation and characterization of 4-*epi*-vancosamine. Tetrahedron Lett. 29: 1223~1226, 1988
19) BATTA, G. & A. LIPTÁK: An approach to oligosaccharide sequencing: 2D N.M.R. DEPT experiment for detection of interglycosidic ^{13}C-^{1}H spin-spin couplings. J. Chem. Soc. Chem. Commun. 1985: 368~370, 1985
20) WERBELOW, L. G. & D. M. GRANT: Intramolecular dipolar relaxation in multispin systems. Adv. Magn. Reson. 9: 189~299, 1977
21) WALTHO, J. P.; D. H. WILLIAMS, D. J. M. STONE & N. J. SKELTON: Intramolecular determinants of conformation and mobility within the antibiotic vancomycin. J. Am. Chem. Soc. 110: 5638~5643, 1988
22) WILLIAMS, D. H.; M. P. WILLIAMSON, D. W. BUTCHER & S. J. HAMMOND: Detailed binding sites of the antibiotics vancomycin and ristocetin A: Determination of intermolecular distances in antibiotic/substrate complexes by use of the time-dependent NOE. J. Am. Chem. Soc. 105: 1332~1339, 1983
23) FESIK, S. W.; T. J. O'DONNELL, R. T. GAMPE, Jr. & E. T. OLEJNICZAK: Determining the structure of a glycopeptide-Ac_2-Lys-D-Ala-D-Ala complex using NMR parameters and molecular modeling. J. Am. Chem. Soc. 108: 3165~3170, 1986
24) HAWKES, G. E.; H. MOLINARI & S. SINGH: A ^{15}N NMR study of intermolecular interactions between vancomycin and Ac-D-Ala-D-Ala. J. Magn. Reson. 74: 188~192, 1987
25) WALTHO, J. P.; J. CAVANAGH & D. H. WILLIAMS: Aspects of molecular recognition: Use of a truncated driven pseudo-NOESY experiment to elucidate the environment of intermolecular electrostatic interactions in vancomycin. J. Chem. Soc. Chem. Commun. 1988: 707~709, 1988
26) KOMÁROMI, I.; Á. SOMOGYI, Z. DINYA, R. BOGNÁR & F. SZTARICSKAI: The role of the carboxylate binding pocket of the vancomycin group of antibiotics in the antibacterial effect. J. Mol. Struct. (Theochem) 201: 351~361, 1989
27) WALTHO, J. P. & D. H. WILLIAMS: Aspects of molecular recognition: Solvent exclusion and dimerization of the antibiotic ristocetin when bound to a model bacterial cell-wall precursor. J. Am. Chem. Soc. 111: 2475~2480, 1989
28) GOOD, V. M.; M. N. GWYNN & D. J. C. KNOWLES: MM 45289, a potent glycopeptide antibiotic which interacts weakly with diacetyl-L-lysyl-D-alanyl-D-alanine. J. Antibiotics 43: 550~555, 1990
29) DIETRICH, W.; C. H. RÜDEL & M. NEUMANN: Fast and precise automatic baseline correction of one- and two-dimensional NMR spectra. J. Magn. Reson. 91: 1~11, 1991